

靶向 DNA 的刚性配体的双核芳基钌配合物

李 季¹ 郝元元¹ 钱 勇¹ 薛旭玲¹ 苏 志^{*,1} 刘红科^{*,1,2}

(¹ 南京师范大学化学与材料科学学院, 江苏生物功能材料重点实验室, 南京 210023)

(² 南京大学化学化工学院, 配位化学国家重点实验室, 南京 210023)

摘要: 以刚性配体 1,3-bib(1,3-二(1*H*-咪唑-1-基)苯)与[Ru(η^6 -*p*-bip)Cl₂]₂(*p*-bip, 联苯基团)为原料, 合成了 3 种双核芳基钌配合物 [Ru₂(η^6 -*p*-bip)₂(1,3-bib)₂XY]X₂ (X=Y=Cl⁻ (**1**), X=Y=Br⁻ (**2**), X=I⁻ 和 Y=Cl⁻ (**3**)), 并用核磁和质谱等对配合物进行了表征。配合物 **1** 的单晶衍射结果表明其具有一种刚性双核 M₂L₂ 碗状结构, 空腔中心有一个阴离子 Cl⁻。配合物 **3** 对 A549 细胞有较高的抗癌活性 (IC₅₀=13.9 μ mol·L⁻¹), 与顺铂细胞毒性 (IC₅₀=15.2 μ mol·L⁻¹) 相当。紫外吸收光谱、圆二色谱、凝胶电泳法研究表明配合物 **1~3** 与 DNA 发生强烈的相互作用并且诱发 DNA 发生解旋。

关键词: 芳基钌; 晶体结构; 抗癌活性; DNA 作用

中图分类号: O614.82[†]

文献标识码: A

文章编号: 1001-4861(2019)08-1500-09

DOI: 10.11862/CJIC.2019.184

DNA Targeting Rigid Dinuclear Ruthenium-Arene Complexes

LI Ji¹ HAO Yuan-Yuan¹ QIAN Yong¹ XUE Xu-Lin¹ SU Zhi^{*,1} LIU Hong-Ke^{*,1,2}

(¹ College of Chemistry and Materials Science, Jiangsu Key Laboratory of Biofunctional Materials, Nanjing Normal University, Nanjing 210023, China)

(² State Key Laboratory of Coordination Chemistry, School of Chemistry and Chemical Engineering, Nanjing University, Nanjing 210023, China)

Abstract: Three dinuclear Ru(II)-arene complexes [Ru₂(η^6 -*p*-bip)₂(1,3-bib)₂XY]X₂ (X=Y=Cl⁻ (**1**), X=Y=Br⁻ (**2**), X=I⁻ and Y=Cl⁻ (**3**); 1,3-bib=1,3-di(1*H*-imidazol-1-yl)benzene, *p*-bip=biphenyl) were synthesized and fully characterized by ¹H NMR and ESI-MS. Single crystal X-ray diffractions studies showed that complex **1** owns a rigid M₂L₂ bowl-like structure, where one Cl⁻ is trapped inside the cavity to balance the charge. Complex **3** showed the best anticancer activities among complexes **1~3**. The IC₅₀ value of **3** towards to human lung cancer cells (A549) reached to 13.9 μ mol·L⁻¹, which is comparable to that of cisplatin (IC₅₀=15.2 μ mol·L⁻¹). Complexes **1~3** have shown strong interactions with DNA and could induce the unwinding of the DNA superhelix structure. CCDC: 1875666, **1**.

Keywords: Ru-arene complexes; crystal structure; anticancer activity; interaction with DNA

0 Introduction

Cisplatin, as the most widely used anticancer drug, has attracted more and more concerns due to the

serious side-effects and resistance^[1-3]. Piano-stool-like metal-arene complexes, especially the Ru(II)-arene complexes, have been considered as the most potent substitutes for the cisplatin, because of their unique

收稿日期: 2019-03-30。收修改稿日期: 2019-05-15。

国家自然科学基金国际合作重点项目(No.21420102002), 国家自然科学基金(No.21601088, 21771109, 21778033)和江苏省自然科学基金(No.BK20171472)资助。

*通信联系人。E-mail: liuhongke@njnu.edu.cn, zhisu@njnu.edu.cn

and versatile biochemical properties^[4-5]. In addition, the multinuclear metal-arene complexes have indicated the enhanced anticancer activities than the corresponding mononuclear complexes^[6-7]. In our previous study, dinuclear Ru(II)-arene complexes based on the rigid imidazole-containing ligand 1,3-di (1*H*-imidazol-1-yl) benzene (1,3-bib) and capped *p*-cymene (*p*-cym) with various counter anions, have shown strong DNA interactions and distinct anticancer behaviors^[8]. As is known, the arene group, as the core component in the metal-arene complex, has important impact on the anticancer activities, which could facilitate the entry of the substrate into cells^[4].

In order to study the effect of arene ligands on the anticancer activities, we changed the arene group from the *p*-cym group to the biphenyl group (*p*-bip), since the *p*-bip has higher hydrophobicity than *p*-cym, which could increase cellular accumulation and the anticancer activity^[9-10]. Three new dinuclear Ru(II)-arene complexes have been synthesized and studied. These complexes were listed as [Ru₂(η⁶-*p*-bip)₂(1,3-bib)₂XY]X₂ (X=Y=Cl⁻ (**1**), X=Y=Br⁻ (**2**), X=I⁻ and Y=Cl⁻ (**3**)) and the single crystal structure of **1** has been resolved. Bowl-like structure of **1** has been observed and one counter anion is included in the center of the structure. Among complexes **1**~**3**, complex **3** indicated the best anticancer activity with IC₅₀ values of 13.9 and 15.2 μmol · L⁻¹ towards HeLa and A549 cancer cells, respectively, due to the existence of the I⁻ anions. Strong interactions between complexes **1**~**3** to DNA have been studied and confirmed by UV-Vis spectra, CD spectra, and gel electrophoresis experiments.

1 Experimental

1.1 Materials and methods

Reactions were carried out under argon by using standard Schlenk techniques. All solvents were of analytical grade. Chemicals were obtained from commercial sources and used without further purification. The ligand 1,3-bib and dimer [RuCl₂(η⁶-*p*-bip)]₂ were synthesized according to the literature methods^[11-12]. Deuterated solvent for NMR purposes were obtained from Merck and Cambridge Isotopes. ¹H

NMR spectra were recorded on a Bruker AVANCE 400 spectrometer at ambient temperature. Electrospray ionization mass spectra (ESI-MS) were obtained using an LCQ spectrometer (Thermo Scientific). A Varian Cary 50 Probe UV-Vis spectrophotometer was used for UV scanning. The circular dichroic spectra of DNA in the region between 200 and 350 nm were obtained by using an Applied-Photophysics Chirascan spectrophotometer operating at 25 °C.

1.2 Syntheses of complexes

1.2.1 [Ru₂(η⁶-*p*-bip)₂(1,3-bib)₂Cl₂]Cl₂ (**1**)

Ligand 1,3-bib (42.0 mg, 0.2 mmol) and Ru₂(η⁶-*p*-bip)₂Cl₄ (65.2 mg, 0.1 mmol) were stirred in 20 mL CH₃OH solution at 65 °C. After refluxing for 12 h under the N₂ protection, the solvent was removed under vacuum and the crude product was further purified by silica gel chromatography using CH₂Cl₂/CH₃OH as the elute. Pale yellow product was collected with a yield of 85% based on the consumed Ru(II) dimer. Elemental analysis Calcd. for Ru₂C₄₈H₄₄Cl₄N₈O₂(%): C 51.99, H 4.00, N 10.10; Found(%): C 51.48, H 3.96, N 10.19. ¹H NMR (DMSO-d₆, 400 MHz): δ 10.31 (s, 4H, 1,3-bib), 8.95 (s, 2H, 1,3-bib), 7.98 (t, 4H, *J*=1.7 Hz, 1,3-bib), 7.85~7.80 (m, 4H, 1,3-bib), 7.70 (d, 6H, *J*=1.5 Hz, 1,3-bib), 7.44~7.36 (m, 10H, *p*-bip), 6.71 (d, 4H, *J*=6.0 Hz, *p*-bip), 6.50 (t, 4H, *J*=6.3, 5.5 Hz, *p*-bip), 6.21 (t, 2H, *J*=5.6 Hz, *p*-bip). ESI-MS(+): Calcd. for [Ru₂(η⁶-*p*-bip)₂(1,3-bib)₂Cl₃]⁺ ([Ru₂C₄₈H₄₀N₈Cl₃]⁺) *m/z*: 1 037.38, Found: 1 039.08; Calcd. for [Ru₂(η⁶-*p*-bip)₂(1,3-bib)₂Cl₂]²⁺ ([Ru₂C₄₈H₄₀N₈Cl₂]²⁺) *m/z*: 500.96, Found: 501.25.

1.2.2 [Ru₂(η⁶-*p*-bip)₂(1,3-bib)₂Br₂]Br₂ (**2**)

To a CH₃OH solution (5 mL) of complex **1** (16.09 mg, 0.015 mmol), 5 mL CH₃OH containing AgCF₃SO₃ (15.42 mg, 0.06 mmol) was added. After stirred for 12 h at room temperature, the AgCl precipitate was removed by filtration, and the CH₃OH solution (15 mL) containing KBr (89.25 mg, 0.75 mmol) was added dropwise to the resulting solution. After 12 h, the solvent was removed under vacuum and the crude product was further purified by silica gel chromatography using CH₂Cl₂/CH₃OH as the eluent. Pale yellow product was collected with a yield of 79% based on the consumed complex **1**. Elemental analysis Calcd. for

$\text{Ru}_2\text{C}_{48}\text{H}_{42}\text{Br}_4\text{N}_8\text{O}(\%)$: C 45.44, H 3.34, N 8.83; Found (%): C 44.99, H 3.31, N 8.90. ^1H NMR ($\text{DMSO}-d_6$, 400 MHz): δ 9.87 (s, 4H, 1,3-bib), 8.78 (s, 2H, 1,3-bib), 7.94 (s, 4H, 1,3-bib), 7.86~7.61 (m, 10H, *p*-bip), 7.53 (s, 4H, *p*-bip), 7.48~7.30 (m, 6H, *p*-bip), 6.78 (d, $J=5.9$ Hz, 4H, *p*-bip), 6.52 (t, $J=5.7$ Hz, 4H, *p*-bip), 6.13 (t, $J=5.5$ Hz, 2H, *p*-bip). ESI-MS(+): Calcd. for $[\text{Ru}_2(\eta^6\text{-}p\text{-bip})_2(1,3\text{-bib})_2\text{Br}_3]^+$ ($[\text{Ru}_2\text{C}_{48}\text{H}_{40}\text{N}_8\text{Br}_3]^+$) m/z : 1 170.74, Found: 1 170.83.

1.2.3 $[\text{Ru}_2(\eta^6\text{-}p\text{-bip})_2(1,3\text{-bib})_2\text{ClI}]\text{I}_2$ (**3**)

To a CH_3OH solution (5 mL) of complex **1** (16.09 mg, 0.015 mmol), 5 mL CH_3OH containing AgCF_3SO_3 (15.42 mg, 0.06 mmol) was added. After stirred for 12 h at room temperature, the AgCl precipitate was removed by filtration, and the CH_3OH solution (15 mL) containing KI (124.50 mg, 0.75 mmol) was added dropwise to the resulting solution. After 12 h, the solvent was removed under vacuum and the crude product was further purified by silica gel chromatography using $\text{CH}_2\text{Cl}_2/\text{CH}_3\text{OH}$ as the eluent. Pale red product was collected with a yield of 80% based on the consumed complex **1**. Elemental analysis Calcd. for $\text{Ru}_2\text{C}_{48}\text{H}_{42}\text{ClI}_3\text{N}_8\text{O}(\%)$: C 42.23, H 3.10, N 8.21; Found(%): C 41.81, H 3.06, N 8.29. ^1H NMR ($\text{DMSO}-$

d_6 , 400 MHz): δ 10.15 (s, 4H, 1,3-bib), 8.81 (s, 2H, 1,3-bib), 7.93 (d, $J=16.6$ Hz, 4H, 1,3-bib), 7.78 (d, $J=6.9$ Hz, 4H, 1,3-bib), 7.75~7.62 (m, 6H, 1,3-bib), 7.44~7.35 (m, 10H, *p*-bip), 6.70 (d, $J=5.9$ Hz, 4H, *p*-bip), 6.47 (t, $J=5.7$ Hz, 4H, *p*-bip), 6.19 (t, $J=5.5$ Hz, 2H, *p*-bip). ESI-MS(+): Calcd. for $[\text{Ru}_2(\eta^6\text{-}p\text{-bip})_2(1,3\text{-bib})_2\text{ClI}_2]^+$ ($[\text{Ru}_2\text{C}_{48}\text{H}_{40}\text{N}_8\text{ClI}_2]^+$) m/z : 1 220.29, Found: 1 220.83.

1.3 X-ray crystallographic study

Diffraction data were collected using a Bruker Apex 2 CCD with $K\alpha$ radiation ($\lambda=0.071\ 073$ nm) at 296(2) K for complex **1** using the ω - 2θ scan method. Absorption corrections were applied using a multi-scan technique^[13]. An empirical absorption correction was applied. All the structures were solved by direct methods using SHELXS-2014 and refined by the full-matrix least-squares techniques using the SHELXL-2014^[14] program within WINGX. All non-hydrogen atoms were refined anisotropically and the hydrogen atoms of the organic molecule were refined at calculated positions, assigned isotropic thermal parameters, and allowed to ride their parent atoms. The crystallographic data and detailed bond distances and angles were listed in Table 1 and 2.

CCDC: 1875666, **1**.

Table 1 Crystallographic data of **1**

Formula	$\text{Ru}_2\text{C}_{48}\text{H}_{44}\text{Cl}_4\text{N}_8\text{O}_2$	$F(000)$	2 240
Formula weight	1 108.85	θ range / (°)	1.2~28.1
Crystal system	Monoclinic	Limiting indices	$-17 \leq h \leq 17, -12 \leq k \leq 12, -45 \leq l \leq 45$
Space group	$P2_1/c$	Reflection collected, unique	35 046, 10 018
a / nm	1.383 13(19)	R_{int}	0.061
b / nm	0.925 39(13)	Completeness to $\theta=25.00^\circ$ / %	92.70
c / nm	3.478 1(5)	Data, restraint, parameter	10 018, 0, 583
β / (°)	94.371(2)	Goodness-of-fit on F^2	1.043
Z	4	Final R indices $[I > 2\sigma(I)]^a$	$R_1=0.048\ 0, wR_2=0.102\ 6$
D_c / ($\text{g}\cdot\text{cm}^{-3}$)	1.659		

$$^a R_1 = \sum ||F_o| - |F_c|| / \sum |F_o|; wR_2 = [\sum w(|F_o|^2 - |F_c|^2)^2 / \sum w(F_o)^2]^{1/2}, \text{ where } w = 1/[\sigma^2(F_o^2) + (aP)^2 + bP], P = (F_o^2 + 2F_c^2)/3.$$

Table 2 Selected bond lengths (nm) and angles (°) for **1**

Ru1-N1	0.210 3(3)	Ru1-Cl1	0.240 9(1)	Ru2-N5	0.209 5(3)
Ru1-N8	0.210 1(3)	Ru2-N4	0.211 1(4)	Ru2-Cl2	0.240 0(1)
N1-Ru1-Cl1	86.47 (8)	N1-Ru1-N8	89.44 (12)	N5-Ru2-Cl2	86.95 (9)
N8-Ru1-Cl1	85.06 (10)	N4-Ru2-Cl2	88.17 (9)	N4-Ru2-N5	87.28(13)

1.4 UV studies

Complexes **1**~**3** were characterized by UV-Vis spectroscopy. All the complexes were dissolved in DMSO/H₂O (1:9, V/V), and the final concentration is 100 $\mu\text{mol}\cdot\text{L}^{-1}$. The absorbance was recorded at time intervals of 1 h at 298 K for 17 h.

1.5 Cell viability assay

HeLa, A549 and LO2 cells were obtained from the Experimental Animal Centre of Sun Yat-Sen University (Guangzhou, China) and cultured in DMEM (Dulbecco's modified Eagle's medium, Gibco BRL) containing 10% FBS (fetal bovine serum, Gibco BRL), 100 $\mu\text{g}\cdot\text{mL}^{-1}$ streptomycin and 100 $\text{U}\cdot\text{mL}^{-1}$ penicillin (Gibco BRL). Cells were grown at 37 $^{\circ}\text{C}$ in a 5%(V/V) CO₂ humidified incubator. The cytotoxicity of the tested complexes towards different cell lines was determined by MTT assay. Cells were cultured in 96-well plates for 24 h. Cells were incubated with a series of concentrations of complexes for another 48 h. 20 μL MTT solution (5 $\text{mg}\cdot\text{mL}^{-1}$) was added into each well and incubated for another 4 h. The culture media was removed and 150 μL DMSO was added into each well. The plate was shaken for 10 min. The absorbance at 492 nm was measured by a microplate reader^[15-16].

1.6 UV-Vis spectroscopy studies of DNA binding property

Calf thymus DNA (CT-DNA) was purchased from Sigma. Phosphate buffer saline (PBS, 5 $\text{mmol}\cdot\text{L}^{-1}$, pH =7.4) was used for the spectral studies on DNA binding properties of the complexes. The PBS was prepared by ultra-pure water at room temperature. The stock CT-DNA solution was stored at 4 $^{\circ}\text{C}$. The concentration of CT-DNA was determined by UV-Vis absorption measurements at 260 nm after proper dilution with PBS buffer, taking 6 600 $\text{L}\cdot\text{mol}^{-1}\cdot\text{cm}^{-1}$ as the molar absorption coefficient. The ratio of UV absorbance (A_{260}/A_{280}) was *ca.* 1.9, indicating that the CT-DNA solution was sufficiently free of protein. Titration experiments were performed at room temperature. The working solution of complexes (100 $\mu\text{mol}\cdot\text{L}^{-1}$) were first placed in a 1 cm path quartz cuvette and aliquots of a CT-DNA stock solution was added, with mixing for 8 min to allow equilibrium to be reached. The

absorption studies were conducted with a fixed complex concentration and alternating the CT-DNA concentration. We observed a subtractive role from each reading on the UV-Vis when the complex and CT-DNA was incubated. With the increasing concentration of CT-DNA, the absorbance change at the metal-to-ligand charge transfer (MLCT) region. The binding constants (K_b) were determined from the spectroscopic titration data with the following equation^[8,17-18]:

$$c_{\text{DNA}}/(\varepsilon_a - \varepsilon_f) = c_{\text{DNA}}/(\varepsilon_b - \varepsilon_f) + 1/[K_b(\varepsilon_b - \varepsilon_f)]$$

where c_{DNA} is the concentration of the DNA; ε_a ($\varepsilon_a = A_{\text{obs}}/c_{\text{complex}}$) is the apparent absorption coefficient; ε_f is the extinction coefficient for the free complex; ε_b stands for the absorption coefficient of the complex when fully bounded to DNA. Linear fitting of $c_{\text{DNA}}/(\varepsilon_a - \varepsilon_f)$ with c_{DNA} from the above equation allowed us to calculate K_b for the complex binding to CT-DNA.

1.7 Circular dichroism spectroscopy studies of DNA binding property

The interaction of complexes with CT-DNA was studied by CD spectroscopy in PBS buffer (50 $\text{mmol}\cdot\text{L}^{-1}$, pH=7.4). A series of samples containing different concentration ratios ($c_{\text{complex}}/c_{\text{DNA}}$) were prepared and incubated at 25 $^{\circ}\text{C}$ for 24 h. The concentration of CT-DNA was set at 100 $\mu\text{mol}\cdot\text{L}^{-1}$ and the ratio increased from 0.02 to 0.12. CD spectra were recorded in the cuvette of 1 cm path length, with the range of 200~350 nm, the scan rate of 100 $\text{nm}\cdot\text{min}^{-1}$ and the slit width of 1 nm.

1.8 Gel electrophoresis experiments

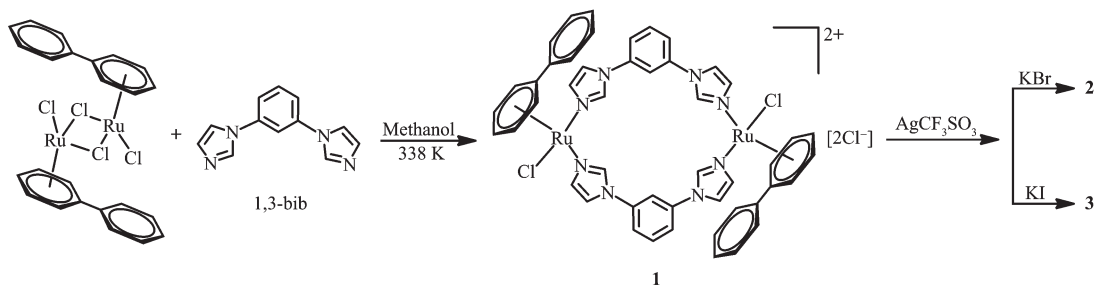
Closed circular supercoiled pBR322 plasmid DNA was used for the gel electrophoresis experiments, which was purchased from Sangon Biotech (Shanghai, China). DNA (1 μL , 200 $\mu\text{mol}\cdot\text{L}^{-1}$) was treated with ultrapure water (4 μL), PBS (5 μL , 100 $\text{mmol}\cdot\text{L}^{-1}$), and different concentrations of complexes (10 μL , $c_{\text{complex}}/c_{\text{DNA}}$ =0.25, 0.5, 0.75, 1.0, 1.5 and 2.0, respectively). The mixture was incubated at 37 $^{\circ}\text{C}$ for 12 h in the dark, then loading buffer (4 μL , 0.05% bromophenol blue, 30 $\text{mmol}\cdot\text{L}^{-1}$ EDTA, 36% glycerol, 0.05% xylene cyanol FF) was added. Electrophoresis was carried out in a native agarose gel (0.8%) in 1×TAE (tris base, acetic acid, and EDTA) buffer for 2 h at 70 mA. The

gel was subsequently stained with $1\ \mu\text{g}\cdot\text{mL}^{-1}$ ethidium bromide and visualized under a UV trans-illuminator and photographed by using a digital camera^[19].

2 Results and discussion

2.1 Design and syntheses of macrocyclic di-ruthenium complexes 1~3

Macrocyclic di-ruthenium complex **1** was obtained from the direct reaction of the ligand (1,3-bib) with the dimer $[\text{Ru}(\eta^6\text{-}p\text{-bip})\text{Cl}_2]_2$, while complexes **2** and **3** were



Scheme 1 Synthetic routes for complexes **1**~**3**

2.2 X-ray crystallography

Complex **1** crystallizes in $P2_1/c$ space group, and shows a classic “bowl-like” macrocyclic structure with Cl^- as the counter anions (Fig.1). Each Ru(II) is coordinated by six carbon atoms from one phenyl ring, two nitrogen atoms from two 1,3-bib ligands and one Cl^- anion. The bond lengths of Ru-N and Ru-Cl are in a range of $0.208\ 6(8)\sim 0.211\ 2(8)\ \text{nm}$ and $0.239\ 8(3)\sim 0.240\ 5(3)\ \text{nm}$, respectively, and the bond angles of N-Ru-Cl and N-Ru-N are in a range of $85.3^\circ\sim 88.4^\circ$ and $87.1(3)^\circ\sim 89.3(3)^\circ$, respectively. The bond lengths and angles are similar to the previously reported Ru(II)-arene complexes^[8,20]. One Cl^- is captured into the bowl-like structure through the hydrogen bonds (Table S1), which is similar to the previously reported complex $[\text{Ru}_2(\eta^6\text{-}p\text{-cymene})_2(1,3\text{-bib})_2\text{Cl}_2](\text{NO}_3)_2$ ^[8]. The trapped Cl^- could be ensured from the results of ESI-MS. For example, for complex **1**, the peak at $1\ 039.08$ was clearly observed for $[\text{Ru}_2(\eta^6\text{-}p\text{-bip})_2(1,3\text{-bib})_2\text{Cl}_3]^+$ (Calcd. m/z : $1\ 037.38$) (Fig.S2)^[8]. The upper and bottom planes of the bowl-like complex **1** are defined by C1, C5, C14 from the arene group and C48, C38 and C33 from the 1,3-bib ligands, respectively (Fig.1a). The diameter of the upper and bottom bases of the “bowl”

prepared by reaction of complex **1** with appropriate silver salts (Scheme 1)^[11]. All complexes were obtained in good yields and characterized by ^1H NMR and ESI-MS (Fig.S1~S4, Supporting Information). In the complex **2**, the coordinated and the counter anions Cl^- were fully replaced by anion Br^- , which were confirmed by the ESI-MS results. However, only one coordinated Cl^- in complex **3** was replaced by a I^- and the formula of $[\text{Ru}_2(\eta^6\text{-}p\text{-bip})_2(1,3\text{-bib})_2\text{ClI}]\text{I}_2$ was confirmed by the ESI-MS results.

were 1.25 or $0.94\ \text{nm}$, with a distance of $0.43\ \text{nm}$ between the two bases. Comparing to $[\text{Ru}_2(\eta^6\text{-}p\text{-cymene})_2(1,3\text{-bib})_2\text{Cl}_2](\text{NO}_3)_2$, complex **1** owned a larger open window ($0.94\ \text{nm}$ vs $0.91\ \text{nm}$) and longer distance between two bases ($0.43\ \text{nm}$ vs $0.4\ \text{nm}$). The Ru1...Ru2 distance is $0.97\ \text{nm}$ in complex **1**. The dinuclear units are further connected by the $\pi\text{-}\pi$ interactions between two paralleled phenyl rings from two adjacent units with the “center-to-center” distances of 0.346 and $0.378\ \text{nm}$, and the dihedral angle of 0° and 4.8° , respectively.

2.3 Cytotoxicity of complexes 1~3 in vitro

The cytotoxicity was evaluated in A549 (human lung cancer), HeLa (human cervical cancer), and LO2 (human normal liver cell line) by the colorimetric MTT assay for 48 h. Cisplatin was also tested as a positive control. The results are listed in Table 3 and show that complexes **1**~**3** own less toxicity to normal human cells (LO2) with an IC_{50} value of 28.5 , 13.6 and $13.0\ \mu\text{mol}\cdot\text{L}^{-1}$, respectively, comparing to the cisplatin with the IC_{50} value of $1.5\ \mu\text{mol}\cdot\text{L}^{-1}$. Among **1**~**3**, complex **3** shows the best anticancer activity to the cancer cells HeLa and A549 with IC_{50} value of 15.2 and $13.9\ \mu\text{mol}\cdot\text{L}^{-1}$, respectively, which is comparable

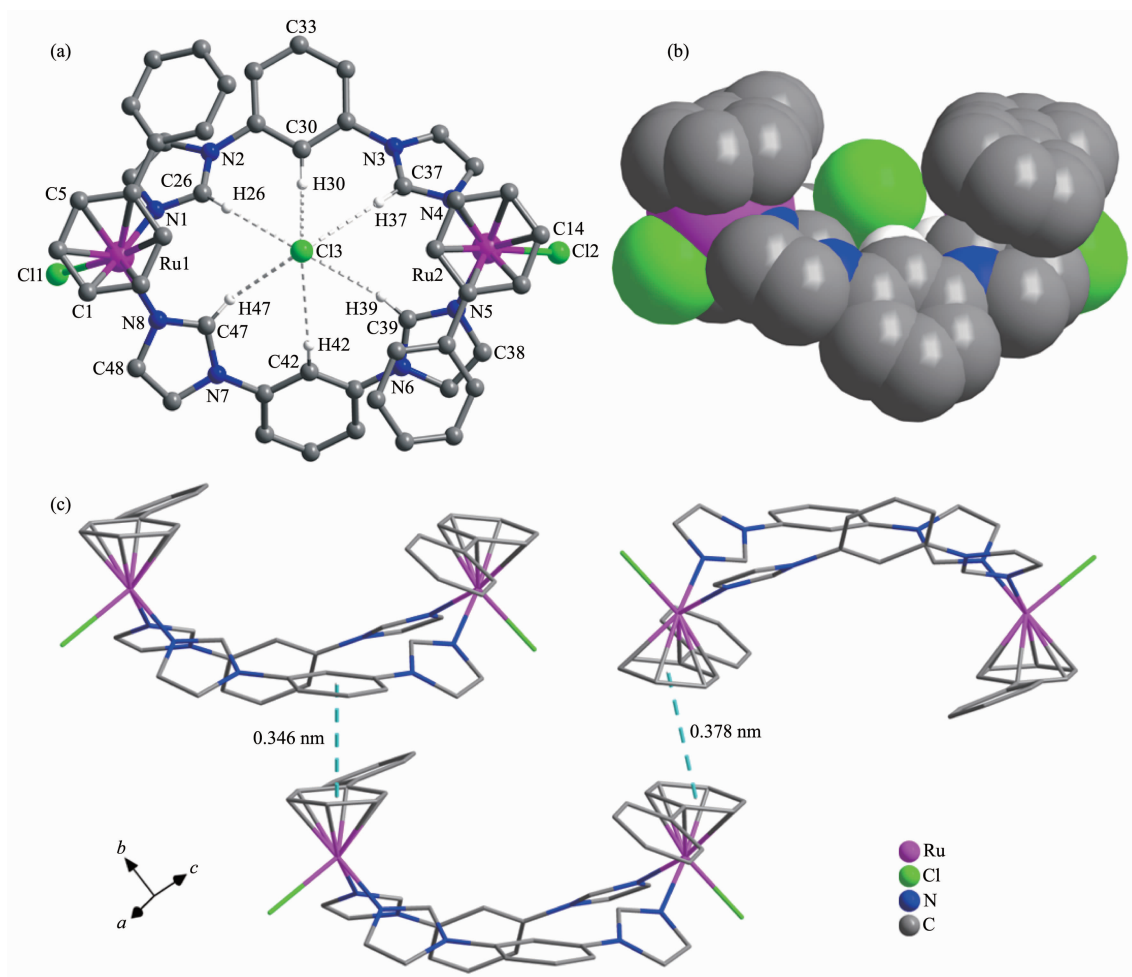


Fig.1 (a) X-ray structure of complex **1**, where one Cl^- anion was enveloped as a guest molecular, and the other Cl^- , partial hydrogen atoms, and the free water molecules are omitted for clarity; (b) Side-viewing of bowl-like complex **1** in space filling mode; (c) π - π stacking interactions between two parallel phenyl rings of two adjacent units, with a “center-to-center” distance of 0.346 and 0.378 nm, respectively

Table 3 IC_{50} values of complexes **1**~**3** as obtained from MTT assay

Compound	$\mu\text{mol} \cdot \text{L}^{-1}$		
	HeLa	A549	LO2
1	25.6±1.7	45.4±2.3	28.5±0.8
2	21.9±2.1	28.9±1.4	13.6±0.8
3	15.2±1.1	13.9±1.1	13.0±0.5
Cisplatin	7.9±0.4	15.2±0.5	1.5±0.1

to that of cisplatin. In general, the anti-proliferative efficacy of dinuclear Ru(II) complexes are in the following order: **3** > **2** > **1**, which indicates the important role of the counter anions, since the halide exchange could modify the cellular uptake and accumulation pathways^[9]. Comparing to the other dinuclear Ru(II)-arene with I^- as the counter anions, $[\text{Ru}_2(\eta^6\text{-}p\text{-cymene})_2(m\text{-bib})_2]\text{I}_2$ ($m\text{-bib}$ = 1,3-bis(1*H*-imidazol-1-yl)methyl)

benzene) and $[\text{Ru}_2(\eta^6\text{-}p\text{-cymene})_2(1,3\text{-bib})_2\text{Cl}_2]\text{I}_2$, complex **3** showed a significant enhancement in the anti-cancer activity to A549 cancer cells with IC_{50} value of $13.9 \mu\text{mol} \cdot \text{L}^{-1}$ vs $150.1 \mu\text{mol} \cdot \text{L}^{-1}$ and $30.9 \mu\text{mol} \cdot \text{L}^{-1}$, respectively^[8,19]. The results here indicate that both the ligand and the arene group play important roles for the enhancement of the anticancer activity of these dinuclear Ru-arene complexes^[9]. In addition, complex

3 exhibits much higher anticancer activity comparing to several reported mononuclear complexes towards A549 cell lines^[21].

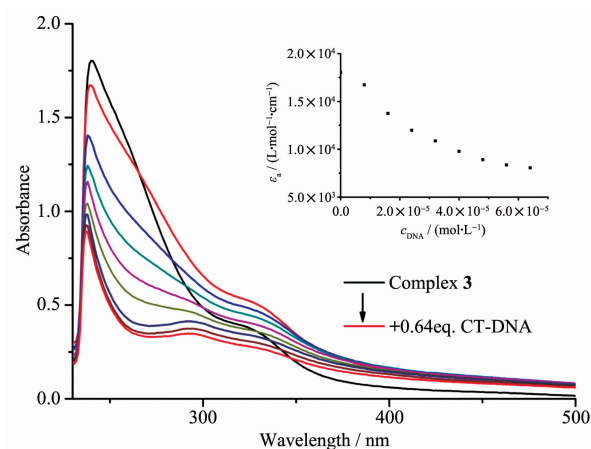
2.4 UV studies

The UV studies of the complex in solution is important for biological application. As shown in Fig. S5, the characteristic absorption bands for the complexes **1** and **2** showed only minimum or no change, while the bands for complex **3** displayed slight hypochromicity, indicating that complexes **1~3** could maintain their structural integrity in aqueous solution at 298 K. Previously reported dinuclear Ru(II)-arene complex with rigid ligand have also showed high stability under physiological conditions^[22-23].

2.5 Interaction with CT DNA

In order to understand the interactions of Ru(II)-arene complexes with potent targets in the cancer cells, especially DNA, the DNA titration experiment was studied by the UV-Vis, CD and DNA electrophoresis.

The UV-Vis spectra of the titration experiments of CT-DNA by complexes **1~3** at 25 °C are shown in Fig.2 and S6. Complex **3** showed a maximum absorption wavelength at 240 nm and it slightly blue-shifted to 237 nm with the addition of 0.66 equal amounts of CT-DNA. The hypochromicity percentage of the MLCT band (metal to ligand charge transfer) was observed to be 50.3% at 241 nm, which suggests the strong stacking interaction between 1,3-bib ligands and the base pairs of DNA^[8]. Similar blue-shift bands were detected for complexes **1** or **2** from 241 to 238 nm or 244 to 242 nm, respectively. The hypochromicity percentage of complexes **1** and **2** were observed much less than that of complex **3**, as 15.1% and 24.1% with the addition of 0.8 and 0.88 equal amount of CT-DNA, respectively, which suggests that complex **3** showed the strongest binding ability to DNA^[24]. The intrinsic binding constants (K_b) of complexes **1~3** to CT-DNA were 1.62×10^4 , 6.27×10^3 and 2.07×10^4 L · mol⁻¹, respectively. Comparing to our previous reported dinuclear Ru(II)-arene complexes with *p*-cymene as the arene group, the binding capacity to DNA has been dramatically decreased, which may result from the substitution of biphenyl group^[25].

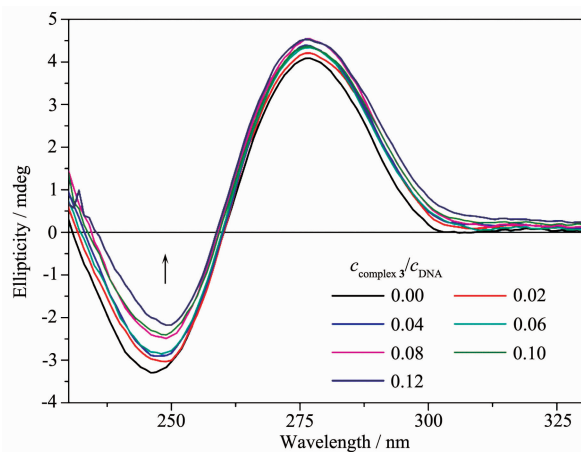


Arrow in the picture shows the absorbance change by the increasing of CT-DNA concentration; Inset: plot of ϵ_a versus c_{DNA} for the titration of DNA with Ru(II) complexes

Fig.2 Absorption spectra of complex **3** in PBS buffer at 25 °C on addition of CT-DNA

To further examine the binding mode between complexes **1~3** with CT-DNA, CD titration experiments were also performed. The positive band at about 278 nm is due to the base stacking and the negative band at about 248 nm is due to the right-handed helicity, which are both the characteristics of B-DNA. The increasing of the ratio of $c_{\text{complex}}/c_{\text{DNA}}$ and dramatic decreasing of the ellipticity for negative bands suggest that **1~3** could unwind the DNA helix and lead to the loss of helicity through rotation of the bases (Fig.3 and S7)^[26].

The effect of the binding of complex **3** on plasmid DNA was also investigated by DNA electrophoresis



Original DNA concentration: 0.1 mmol · L⁻¹

Fig.3 CD spectra of CT-DNA bound by **3** with $c_{\text{complex}}/c_{\text{DNA}}$ ratio ranging from 0 to 0.12

studies. Closed circular DNA can reduce its superhelical density and decrease the DNA migration rate in agarose by binding of unwinding agents^[27]. Positive charged metal complexes could bind to the negative charge part of DNA^[27-28]. Complex **3** induced significant changes in the migration of DNA (Form I) at $2.5 \mu\text{mol} \cdot \text{L}^{-1}$ (Fig.4), suggesting that complex **3** could unwind the DNA superhelix.

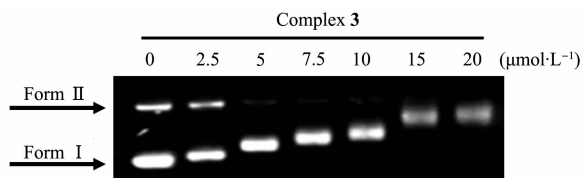


Fig.4 Gel electrophoresis assay of pBR322 DNA treated with complex **3** with variable concentrations

Comparing complexes **1~3** with other dinuclear $[\text{Ru}_2(\eta^6\text{-}p\text{-cymene})_2(1,3\text{-bib})_2\text{Cl}_2]\text{X}_2$ complexes ($\text{X}=\text{Cl}^-$, I^- , NO_3^- , BF_4^- , PF_6^- , CF_3SO_3^-)^[8], even all complexes share the similar bowl-like structure, the best cytotoxicity to A549 cancer cell among complexes **1~3** ($13.9 \mu\text{mol} \cdot \text{L}^{-1}$) is much better than that of $\text{Ru}-\eta^6\text{-}p\text{-cymene}$ complexes ($30.9 \mu\text{mol} \cdot \text{L}^{-1}$)^[8]. In addition, even all complexes could interact with DNA, the binding capacity of complexes **1~3** ($\sim 10^4 \text{ L} \cdot \text{mol}^{-1}$) is much weaker than that of $\text{Ru}-\eta^6\text{-}p\text{-cymene}$ complexes ($\sim 10^5 \text{ L} \cdot \text{mol}^{-1}$). The differences may result from the effect of distinct arene groups ($\eta^6\text{-}p\text{-cymene}$ vs biphenyl).

3 Conclusions

In summary, three $\text{Ru}(\text{II})$ -arene complexes containing the rigid imidazole ligand with distinct counter anions were successfully synthesized and characterized. The single crystal diffraction displays that one counter anion Cl^- could locate in the cavity of dinuclear structure of complex **1**. The cytotoxicity assay indicates that complex **3** exhibits the best cytotoxicity toward to A549 cell line, which is comparable to that of cisplatin. All three complexes show strong interactions with CT-DNA and could unwind the DNA superhelix. The different anticancer behaviors of **1~3** suggest that the coordinative and counter anions and the arene groups in the metal-arene complexes might play very important roles to adjust their anticancer capacities.

Further studies will be continued and focused on the mechanism of the anticancer activity of these $\text{Ru}(\text{II})$ -arene complexes.

Supporting information is available at <http://www.wjhxsb.cn>

References:

- [1] Wang X, Wang X, Jin S, et al. *Chem. Rev.*, **2019**,**119**(2): 1138-1192
- [2] Bergamo A, Dyson P J, Sava G. *Coord. Chem. Rev.*, **2018**, **360**:17-33
- [3] Johnstone T C, Suntharalingam K, Lippard S J. *Chem. Rev.*, **2016**,**116**(5):3436-3486
- [4] Zeng L, Gupta P, Chen Y, et al. *Chem. Soc. Rev.*, **2017**,**46** (19):5771-5804
- [5] Liu H K, Kosthunova H, Habtemariam A, et al. *Dalton Trans.*, **2016**,**45**(46):18676-18688
- [6] Fu Y, Romero M J, Salassa L, et al. *Angew. Chem. Int. Ed.*, **2016**,**55**(31):8909-8912
- [7] Davey G E, Adhireksan Z, Ma Z, et al. *Nat. Commun.*, **2017**, **8**:1575
- [8] Wu Q, Liu L Y, Li S, et al. *J. Inorg. Biochem.*, **2018**,**189**:30-39
- [9] Coverdale J P C, Bridgewater H E, Song J I, et al. *J. Med. Chem.*, **2018**,**61**(20):9246-9255
- [10] Liu H K, Sadler P J. *Acc. Chem. Res.*, **2011**,**44**(5):349-359
- [11] Peacock A F A, Habtemariam A, Fernandez R, et al. *J. Am. Chem. Soc.*, **2006**,**128**(5):1739-1748
- [12] Tronier A, Strassner T. *Dalton Trans.*, **2013**,**42**(27):9847-9851
- [13] ZHANG Fu-Xing(张复兴), HE Tang-Feng(何唐锋), YAO Shu-Fen(姚淑芬), et al. *Chinese J. Inorg. Chem.*(无机化学学报), **2019**,**35**(4):598-604
- [14] Sheldrick G M. *Acta Crystallogr. Sect. A: Found. Crystallogr.*, **2015**,**A71**:3-8
- [15] Guan R, Chen Y, Zeng L, et al. *Chem. Sci.*, **2018**,**9**(23): 5183-5190
- [16] GAO Aan-Li(高安丽), XIONG Qing-Feng(熊庆丰), JIANG Jing(姜婧), et al. *Chinese J. Inorg. Chem.*(无机化学学报), **2018**,**34**(9):1649-1654
- [17] Kumar C V, Barton J K, Turro N J. *J. Am. Chem. Soc.*, **1985**, **107**(19):5518-5523
- [18] MO Hui-Wen(莫慧雯), LIU Ya-Xian(刘雅娴), CAI Dai-Hong(蔡戴宏), et al. *Chinese J. Inorg. Chem.*(无机化学学报), **2019**,**35**(3):477-484
- [19] Wang H Y, Qian Y, Wang F X, et al. *Eur. J. Inorg. Chem.*, **2017**(12):1792-1799

- [20] Li J, Zhang P, Xu Y, et al. *Dalton Trans.*, **2017**, **46**(46):16205-16215
- [21] Clavel C M, Paunescu E, Nowak-Sliwinska P, et al. *Chem. Sci.*, **2014**, **5**(3):1097-1101
- [22] Murray B S, Menin L, Scopelliti R, et al. *Chem. Sci.*, **2014**, **5**(6):2536-2545
- [23] Jeyalakshmi K, Haribabu J, Balachandran C, et al. *Organometallics*, **2019**, **38**(4):753-770
- [24] Zhou W, Wang X, Hu M, et al. *Chem. Sci.*, **2014**, **5**(7):2761-2770
- [25] Li J, Tian M, Tian Z, et al. *Inorg. Chem.*, **2018**, **57**(4):1705-1716
- [26] Karidi K, Garoufis A, Hadjiliadis N, et al. *Dalton Trans.*, **2005**(4):728-734
- [27] Zhu Z, Wang X, Li T, et al. *Angew. Chem. Int. Ed.*, **2014**, **53**(48):13225-13228
- [28] Keck M V, Lippard S J. *Tetrahedron Lett.*, **1993**, **34**(9):1415-1416